



## **Radiological Hazards in Soil from the Bauxite Deposits Sites in Dschang Region of Cameroon**

**M. M. Ndontchueng<sup>1,2\*</sup>, E. J. M. Nguelem<sup>1,2</sup>, O. Motapon<sup>2</sup>, R. L. Njinga<sup>1</sup>,  
A. Simo<sup>1</sup>, J. C. S. Guembou<sup>2</sup> and B. Yimele<sup>1</sup>**

<sup>1</sup>National Radiation Protection Agency of Cameroon, P.O.Box 33732, Yaounde, Cameroon.

<sup>2</sup>Department of Physics, Faculty of Science, University of Douala, P.O.Box 24157, Douala, Cameroon.

### **Authors' contributions**

*This work was carried out in collaboration between all authors. All authors read and approved the final manuscript.*

### **Article Information**

DOI: 10.9734/BJAST/2015/13352

Editor(s):

(1) Vyacheslav O Vakhnenko, Division of Geodynamics of Explosion, Subbotin Institute of Geophysics, National Academy of Sciences of Ukrainian, Ukraine.

Reviewers:

(1) Anonymous, Obafemi Awolowo University, Nigeria.

(2) Anonymous, Agricultural University, Plovdiv, Bulgaria.

(3) M A Saeed, Department of Physics, Faculty of Science, Universiti Teknologi Malaysia, Johor Bahru, Malaysia.

Peer review History: <http://www.sciencedomain.org/review-history.php?iid=761&id=5&aid=6644>

**Original Research Article**

**Received 13<sup>th</sup> August 2014**  
**Accepted 23<sup>rd</sup> September 2014**  
**Published 23<sup>rd</sup> October 2014**

### **ABSTRACT**

This work evaluates the radiological health risk from NORM exposure in bauxite deposition sites of West Region in Cameroon. In-situ and laboratory measurements were performed using dose rate survey meter and Broad Energy Germanium (BEGe) detector. Radiometric analysis of <sup>226</sup>Ra, <sup>232</sup>Th and <sup>40</sup>K in the soil samples from Fongo-Tongo and Mini-Matap were done with average activity concentration of 108.91 Bq/kg, 117.79 Bq/kg and 143.07 Bq/kg and, 113.15Bq/kg, 196.14 Bq/kg and zero were determined respectively. In-situ measurement of dose rate at 1 m above the ground and the annual effective dose values due to <sup>226</sup>Ra, <sup>232</sup>Th and <sup>40</sup>K in 5 cm soil layer were determined using conversion factors by UNSCEAR. The average external hazard indexes in samples from Fongo-Tongo were 0.78 and 1.06 while the internal hazard indexes in samples from Mini-Matap were 1.07 and 1.37. Comparing these values with the worldwide values set by UNSCEAR we realized that avoidance of high exposure from gamma radiation due to NORM to the populace should be of concern.

\*Corresponding author: E-mail: [ndomomau@yahoo.fr](mailto:ndomomau@yahoo.fr);

*Keywords: Gamma radiation; radionuclides; radiological risk; BEGe detector; soil.*

## 1. INTRODUCTION

Bauxites are lateritic or karsts rocks with more than 40% of  $Al_2O_3$  and less than 8% of  $SiO_2$  from which aluminium is obtained Bardossy et al. [1]. World bauxite resources are estimated around 75 billion tons Lee Bray [2], mainly in Africa (33%), Oceania (24%), South America and the Caribbean (22%) and Asia (15%). In West and Central Africa, lateritic bauxites are widespread especially in Guinea, Mali, Burkina-Faso, Ivory-Cost, Ghana, Nigeria and Cameroon with an estimation of more than 60 ores deposits Kobilseck [3]. Most of the bauxite deposits in Europe belong to the karsts type and located in Southern Europe along the Mediterranean Sea and in the Ural Mountain. The lateritic bauxite deposits in Europe occur on the Russia platform, in Poland, Northern Ireland and in Turkey. The amount of bauxite found in Russia account about 2% of worldwide resources.

In Cameroon, works on lateritic bauxites started in the early 20<sup>th</sup> century Edlinger et al. [4]; Passarge et al. [5,6,7,8,9,10]. Cameroon has the 6<sup>th</sup> world bauxite reserves with approximately 1.5 billion tons and many non explored bauxitic indices published by Weeksteen [6]. The recent geological map shows that the two zones; Fongo-Tongo and Mini-Martap in Dshang Region of Cameroon contain large bauxitic indices which are yet to be exploited.

These bauxites mineral deposition zones may contain high level of NORM that may cause significant health effects to people living around and the workers of the mines. Thus, determination of NORM in the bauxites mineral deposits zones are of importance since long term exposure to high background of NORM might lead to serious health hazards Ndontchueng et al. [11,12]. The population in these areas make use of sundry bricks for building and constructions by using the soil. This work seeks to determine the background level of NORM in aforementioned zones in Dshang Region of Cameroon for the population living around and decision makers to be aware of the radiation background level. It is also aimed at providing a global and national picture of NORM distributions in the areas for urgent control of high radiation risks to the population that may result from NORM.

### 1.1 Geological Setting

The study areas are deeply dissected by a dense hydrographic network which belongs to the Ménoua watershed. The zones are under sub-equatorial climate of high altitude characterized by long rainy season from March to October and short dry season from November to February. The mean annual rainfall is 1755 mm and the average annual temperature is 20°C Momo et al. [13].

The study sites is located on the southern flank of the Bambouto Mountains, a volcanic cone which belongs to the major North-East trending tectonic lineament known as the Cameroon Volcanic Line (CVL). The region consists essentially of thick sequence of trachytic flows, phonolitic plugs/sills, ash-flow tuffs and basaltic flows of Tertiary age which overlie the precambrian crystalline basement. The collapse of the caldera crest resulted in the tilting towards the northwest of this volcanic sequence.

Two discrete bauxitization stages are found in the region. The first is the saprolite cap which was largely eroded during the collapse of the Bambouto caldera. A fraction of the resulting detrital material accumulated down slope on the trachytic flows which forms tiny deposits. This saprolite has a relic trachytic texture with cryptocrystalline gibbsite aggregates pseudomorphous after euhedral sanidine crystals. The second bauxitization stage developed residual lateritic bauxite which forms the Fongo-Tongo deposit. This bauxite overlies the soft mottled clay horizon which shows gradual increase with depth of kaolinite and corresponding decrease of gibbsite. The basal d-spacing of kaolinite also increases with depth and successively replaced by hydrated kaolinite, metahalloysite, and hydrated halloysite. The two types of bauxites are dominantly composed of gibbsite, minor to trace goethite, koalinite, anatase, maghemite, and quartz Momo et al. [13].

## 2. MATERIALS AND METHODS

Thirteen soil samples were randomly chosen in the study zones. Ten of the samples were obtained from Fongo-Tongo zone and three from Mini-Matap zone. Each of the composite soil samples (mixed thoroughly) were collected from

five subsamples in an area of approximately 1 m<sup>2</sup> and a typical depth of about 15 cm from the top surface layer. Each of the composite samples was packed in a secure polyethylene bag to prevent contamination. In order to cover each study zone and to observe a significant local spatial variation in terrestrial radioactivity, the sampling points at each site of the study area were selected at a minimum distance of 400 m from one another. Each sampling point was marked using a global positioning system (GPS) as shown in Table 1. The samples were transferred into the laboratory after they were labelled accordingly.

At the laboratory, the samples were air dried in an oven for 24 h at a temperature of 105°C. The dried samples were grinded into powder and sieved through a 2 mm wire mesh to obtain a homogenous particles size. In order to achieve radioactive equilibrium between parents and its daughters, the soil samples were then packed in a 120 ml air tight polyethylene cylindrical container, dry-weighed and stored for 32 days to attained secular equilibrium between the long-lived parent and daughter nuclides.

## 2.1 Samples Measurement

Each sample was subjected to a coaxial gamma-ray spectrometer consisting of Broad Energy Germanium (BEGe-6530) Detector manufactured by Canberra Industries in Vienna. The resolution of this detector is 0.5 keV at 5.9 keV for <sup>55</sup>Fe, 0.75 keV at 122 keV for <sup>57</sup>Co and 2.2 keV at 1332 keV for <sup>60</sup>Co. The detector is placed in a low-level Canberra Model 747 lead shield with thickness of 10 cm. Each sample was counted for 86400 sec for effective peak area statistics of above 0.1%. Following the sample analysis process, the specific activity concentration for each radionuclide were calculated automatically by Genie-2000 software based on the equation published by Ndontchueng et al. [12].

## 2.2 Coincidence Summing Correction Factor

Coincidence summing is due to the simultaneous detection of two or more gamma-rays occurring in cascade from the decay of an excited nucleus in which the lifetimes of intermediate levels are short relative to the integration time of the amplifier. The coincidence summing correction factor applied using this study depends on the nuclide decay scheme, the sample geometry and

composition, and the detector features. This becomes relevant for close source-to-detector configuration of the counting geometry, like in the case of MCA\_BEGe-6530 system used and need to be considered when working on NORM (U and Th-series) due to the appearance of the cascade summing in their decay chain. In order to correct for summing during the study, the total efficiency was obtained by calculating the peak-to-total ratio (P/T) defined as the net count in the main peak of the nuclide to the total counts obtained in the spectrum (with background subtraction applied).

## 2.3 Geometry Composer and Efficiency Calibration

Before generating the efficiency curve, the calibration file was defined. This was generated by the Canberra designed Laboratory Sourceless Object Counting System (LabSOCS) which is a mathematical calibration software that incorporates the characterization information of the BEGe-6530 detector in collaboration with Canberra laboratory in Austria. When generating the efficiency calibration file, the LabSOCS calibration software takes into account all parameters related to these measurements including dimensions of the counting geometries, physical and chemical compositions as well as the distance source-to-detector end-cap. To validate the accuracy of the LabSOCS mathematical efficiency calibration, some test were conducted comparing the LabSOCS generated efficiency results with the empirical peak efficiency for a <sup>60</sup>Co point source positioned at a distance of 25 cm from the detector end-cap and the results agreed perfectly.

## 2.4 Spectra Analysis

Genie 2000, Gamma Acquisition Version 3.2.1 and Gamma Analysis Software Version 3.2.3 were used for data acquisition and analysis automatically check and perform the interference correction and calculate the weighted mean of the radionuclide emitting more than one gamma ray. The specific activity concentrations of each radionuclide were identified as follows;

- a) <sup>226</sup>Ra concentration was calculated as a weighted mean of the activity concentrations of the gamma-rays of <sup>214</sup>Pb (351.9 keV), <sup>214</sup>Bi (609.3 keV) and its specific gamma-ray at 186.2 keV. Interference correction due to the presence of 185.7 keV energy peak of <sup>235</sup>U was

taken into account and subtracted accordingly.

- b) The gamma-ray photo-peaks used for the determination of the  $^{232}\text{Th}$  contents were 338.4 keV, 911.2 keV and 969.11 keV of  $^{228}\text{Ac}$  and 238.6 keV of  $^{212}\text{Pb}$ .
- c)  $^{40}\text{K}$  was directly determined by using 1460.8 keV gamma-ray.

## 2.5 Health Hazard Parameters

In order to assess radiation dose received by population living around the investigated areas, some health hazard parameters were evaluated and displayed as follow:

### 2.5.1 Absorbed dose rate in air (*D*)

#### 2.5.1.1 In-situ measurement of absorbed dose rate in air

The *In-situ* measurement of the absorbed dose rate in air at 1 m above the ground were recorded using a dose rate survey meter Radiagem 2000 manufacturer by CANBERRA which was calibrated before usage. It has the ability to measure gamma radiation range of 3  $\mu\text{Sv/h}$  to 100  $\text{mSv/h}$  and the energy range of 40 keV to 125 MeV.

#### 2.5.1.2 Experimental absorbed dose rate in air

The radioactivity concentrations of natural radionuclides and their exposure in air at 1 m above the ground surface are known as the absorbed dose rate. The mean activity concentrations of  $^{226}\text{Ra}$  (of the  $^{238}\text{U}$  series),  $^{232}\text{Th}$ , and  $^{40}\text{K}$  ( $\text{Bq kg}^{-1}$ ) in the soil samples were used to calculate the absorbed dose rate using the following formula provided by European Commission [14].

$$D (\text{nGy.h}^{-1}) = 0.92A_{\text{Ra}} + 1.1A_{\text{Th}} + 0.08A_{\text{K}} \quad (1)$$

where *D* is the absorbed dose rate in  $\text{nGy.h}^{-1}$ ,  $A_{\text{Ra}}$ ,  $A_{\text{Th}}$  and  $A_{\text{K}}$  are the activity concentration of  $^{226}\text{Ra}$  ( $^{238}\text{U}$ ),  $^{232}\text{Th}$  and  $^{40}\text{K}$ , respectively. The dose coefficients in units of  $\text{nGy.h}^{-1}$  per  $\text{Bq.kg}^{-1}$  were taken from European Commission (EC) [14,15].

### 2.5.2 Annual effective dose equivalent (AEDE)

The absorbed dose rate in air at 1 m above the ground surface does not directly provide the radiological risk to which an individual is exposed Beretka et al. [16]. The absorbed dose can be considered in terms of the annual effective dose equivalent from outdoor and indoor terrestrial

gamma radiation which is converted from the absorbed dose by taking into account two factors namely, the conversion coefficient from absorbed dose in air to effective dose, the outdoor and indoor occupancy factor. The total annual effective dose equivalent can be estimated using the following formula Damla et al. [17] and Ndontchueng et al. [11,12]:

$$AEDE (\text{mSv.y}^{-1}) = AEDE_{\text{outdoor}} + AEDE_{\text{indoor}} \quad (2)$$

### 2.5.3 Radium equivalent activity

As a result of the non uniformity in the distribution of natural radionuclides in the soil samples, the actual activity level of  $^{226}\text{Ra}$ ,  $^{232}\text{Th}$  and  $^{40}\text{K}$  in the samples were evaluated by means of a common radiological index called radium equivalent activity ( $Ra_{\text{eq}}$ ). This was done using the Equation obtained from Beretka and Mathew [16]; Al-Hamarneh and Awadallah [18].

$$Ra_{\text{eq}} (\text{Bq.kg}^{-1}) = A_{\text{Ra}} + 1.43A_{\text{Th}} + 0.077A_{\text{K}} \quad (3)$$

where  $A_{\text{Ra}}$ ,  $A_{\text{Th}}$  and  $A_{\text{K}}$  are the activity concentration of  $^{226}\text{Ra}$ ,  $^{232}\text{Th}$  and  $^{40}\text{K}$  in  $\text{Bq.kg}^{-1}$ , respectively.

### 2.5.4 External and internal hazard indices

Many natural radionuclides in terrestrial soils and rocks upon decay produce an external radiation field to which all human beings are exposed. In terms of dose, the principal primordial radionuclides are  $^{232}\text{Th}$ ,  $^{238}\text{U}$  and  $^{40}\text{K}$ . The decay of these radionuclides in soil produces a gamma-beta radiation field in soil that crosses the soil-air interface to produce exposures to humans. The main factors which determine the exposure rate to a particular individual due to the concentrations of radionuclides in the soil depends on the time spent outdoors. To limit the radiation exposure in the samples to the permissible dose equivalent limit of  $1.00 \text{ mSv.y}^{-1}$ , the external hazard index based on a criterion have been introduced using a model proposed by Krieger [19] which is given by UNSCEAR [20].

$$H_{\text{ex}} = \frac{A_{\text{Ra}}}{370} + \frac{A_{\text{Th}}}{259} + \frac{A_{\text{K}}}{4810} \leq 1 \quad (4)$$

In order to keep the radiation hazard insignificant, the value of external hazard index must not exceed the limit of unity. The maximum value of  $H_{\text{ex}}$  equal to unity corresponds to the upper limit of radium equivalent activity of  $370.00 \text{ Bq.kg}^{-1}$  Turhan et al. [21].

In addition to the external hazard, radon and its short-lived products are also hazardous to the repository organs. To account for this threat the maximum permissible concentration for  $^{226}\text{Ra}$  must be reduced to half of the normal limit ( $185.00 \text{ Bq.kg}^{-1}$ ). The internal exposure to carcinogenic radon and its short-lived progeny is quantified by the internal hazard index ( $H_{in}$ ) given by the expression published by Murty et al. [22].

$$H_{in} = \frac{A_{Ra}}{185} + \frac{A_{Th}}{259} + \frac{A_K}{4810} \leq 1 \quad (5)$$

### 3. RESULTS AND DISCUSSION

The specific activity concentrations of  $^{226}\text{Ra}$ ,  $^{232}\text{Th}$ ,  $^{40}\text{K}$  and radium equivalent in soil samples from Fongo-Tongo and Mini-Matap zone are in Table 1. The radiological hazard parameters obtained from the *In-Situ* measurements and the calculated radiation hazard parameters from the specific activity concentration of  $^{226}\text{Ra}$ ,  $^{232}\text{Th}$  and  $^{40}\text{K}$  in samples from Fongo-Tongo and Mini-Matap areas are presented in Table 2.

As shown in Table 1, the specific activity in soil samples from Fongo-Tongo varied from 56.56 to 176.14 Bq/kg with a mean of 108.91 Bq/kg for  $^{226}\text{Ra}$ , from 82.54 to 177.78 Bq/kg with an average of 117.79 Bq/kg for  $^{232}\text{Th}$  respectively. Similar variation of  $^{226}\text{Ra}$  and  $^{232}\text{Th}$  in soil samples from Mini-Matap were observed. These were varied from 102.69 to 124.42 Bq/kg with average of 113.15 Bq/kg and from 163.22 to 239.96 Bq/kg with an average of 196.14 Bq/kg respectively.

The specific activity of  $^{40}\text{K}$  in soil ranged from 51.10 to 1379.62 Bq/kg with an average of 143.07 Bq/kg for samples from Fongo-Tongo zone. Most of the specific activity of  $^{40}\text{K}$  were found to be below the detection limit (BDL) in all samples from Mini-matap area. It is known that potassium is present in almost all geological and raw material. However, it was not detected in almost all samples from Fongo-Tongo and Mini-matap except two soil samples referred as FT1 and FT9. This was very obvious because BEGe-detector exhibits high background than typical coaxial detectors and is more transparent to high energy cosmogenic background radiation which permeates above background levels in laboratories including high energy gamma from naturally occurring radioisotopes such as  $^{40}\text{K}$ .

The evaluated values of  $R_{eq}$  are summarized in Table 1. The calculated radium equivalent

ranged between 186.18 and 430.37 Bq/kg with a mean of 288.35 Bq/kg for soil samples from Fongo-Tongo and from 336.09 to 467.55 Bq/kg with average of 393.63 Bq/kg for samples from Mini-matap, respectively.

Comparing the variation of specific activity concentrations of  $^{226}\text{Ra}$ ,  $^{232}\text{Th}$ ,  $^{40}\text{K}$  and the radium equivalent activity with the worldwide range values, the observed values of  $^{226}\text{Ra}$  and  $^{232}\text{Th}$  in soil samples from both areas were higher than the reported values of  $^{226}\text{Ra}$  and  $^{232}\text{Th}$  by UNSCEAR [20]. A similar comparison of the obtained average values of  $^{226}\text{Ra}$  and  $^{232}\text{Th}$  in soil samples from Fongo-Tongo and Mini-matap areas with the world population weighted safe limits of UNSCEAR [20] are shown in Table 1. The obtained average value of radium equivalent in samples from Fongo-Tongo were lower than the recommended values of UNSCEAR [20] while the obtained average values in samples from Mini-matap were higher than the safe values of UNSCEAR [20].

The observed activity concentrations of  $^{226}\text{Ra}$ ,  $^{232}\text{Th}$  and  $^{40}\text{K}$  in the present work were compared with other published values obtained from the literature of radioactivity in soil by many authors as dispatched in Table 3. The obtained average activity concentrations of  $^{226}\text{Ra}$  and  $^{232}\text{Th}$  in both studied sites were comparably higher than the values published by other authors with the exception of the recorded average value of  $^{226}\text{Ra}$  in China (Xiaz-hung area) published by Yang et al. [23] which was relatively high than the value obtained in Fongo-Tongo. Similar observations were done for  $^{40}\text{K}$  recorded activity concentration in the present study. It can be seen that the average values of  $^{40}\text{K}$  recorded in the present study were slightly lower than the published values recorded in the selected published data except the average values published by Ndontchueng et al. [12]. When comparing with the published data in soil at different depth from mining regions of East Rhodopes in Bulgaria by Hristov et al. [24] using a gamma-spectrometer with HPGe detector, it can be seen that the obtained results of  $^{226}\text{Ra}$  ( $^{238}\text{U}$ ),  $^{232}\text{Th}$  were higher while those of  $^{40}\text{K}$  were lower with the exception of the value obtained in samples referred. The present values were compared favourably with the recorded average values published by other countries selected from the worldwide investigation of natural radioactivity in soil.

**Table 1. Specific activity concentration of  $^{226}\text{Ra}$ ,  $^{232}\text{Th}$ ,  $^{40}\text{K}$  and radium equivalent in soil samples from Fongo-Tongo and Min-Matap**

Study site	Sample ID	(Bq/kg)				Latitude	Longitude
		Ra-226	Th-232	K-40	Ra <sub>eq</sub>		
Fongo-Tongo	FT1	65.71±3.11	128.36±7.46	51.10±9.54	253.20	05°31'53.2"N	09°58'37.0"W
	FT2	162.53±17.88	107.13±4.08	BDL	315.73	05°31'51.6"N	09°58'35.2"W
	FT3	68.15±4.44	82.54±3.49	BDL	186.18	05°31'49.3"N	09°58'35.4"W
	FT4	95.94±3.89	161.29±11.39	BDL	326.58	05°31'46.8"N	09°58'33.1"W
	FT5	160.51±18.77	134.43±5.00	BDL	352.74	05°31'46.4"N	09°58'35.4"W
	FT6	103.76±5.22	88.74±4.56	BDL	230.66	05°31'47.6"N	09°58'29.0"W
	FT7	111.82±5.74	102.28±5.27	BDL	258.08	05°31'49.2"N	09°38'29.9"W
	FT8	87.93±3.54	86.57±3.97	BDL	211.73	05°31'49.9"N	09°58'31.4"W
	FT9	56.56±2.47	108.73±4.25	1379.62±37.22	318.27	05°31'50.7"N	09°58'35.7"W
	FT10	176.14±14.90	177.78±12.58	BDL	430.37	05°31'53.2"N	09°58'36.9"W
	Average	108.91	117.79	143.07	288.35		
St.Dev.	43.42	32.28	434.78	73.95			
Median	99.85	107.93	0.00	286.90			
Mini-Matap	MM01	112.35±7.85	185.24±7.06	BDL	377.24	05°32'40.4"N	09°59'45.3"W
	MM02	124.41±5.34	239.96±9.01	BDL	467.55	05°32'38.6"N	09°59'24.2"W
	MM03	102.69±5.41	163.22±7.01	BDL	336.09	05°32'33.5"N	09°51'07.1"W
	Average	113.15	196.14		393.63		
	St.Dev.	10.88	39.51	0.00	67.24		
Median	112.35	185.24	0.00	377.24			
Worldwide	Range	17.00-60.00	11.00-68.00	140 -850	-		
	average	35.00	30.00	400.00	370.00		

**Table 2. *In-situ* and laboratory measurements of hazard parameters in soil samples from Fongo-Tongo and Mini-Matap areas**

Sample ID	<i>In situ</i> measurement		Derived radiological indices			
	AD (nGy.h <sup>-1</sup> )	AED (mSv/year)	AD (nGy.h <sup>-1</sup> )	AED (mSv/year)	Hex	Hin
FT1	50.00	0.31	110.02	0.68	0.68	0.86
FT2	80.00	0.49	139.80	0.86	0.85	1.29
FT3	50.00	0.31	81.34	0.50	0.50	0.69
FT4	70.00	0.43	141.74	0.87	0.88	1.14
FT5	90.00	0.55	155.35	0.95	0.95	1.39
FT6	80.00	0.49	101.54	0.62	0.62	0.90
FT7	70.00	0.43	113.44	0.70	0.70	1.00
FT8	80.00	0.49	92.91	0.57	0.57	0.81
FT9	80.00	0.49	149.33	0.92	0.86	1.01
FT10	80.00	0.49	188.76	1.16	1.16	1.64
Average	73.00	0.45	127.42	0.78	0.78	1.07
St.Dev.	13.37	0.08	33.10	0.20	0.20	0.29
Median	80.00	0.49	126.62	0.78	0.78	1.01
MM1	110.00	0.67	163.79	1.01	1.02	1.32
MM2	120.00	0.74	202.41	1.24	1.26	1.60
MM3	160.00	0.98	146.03	0.90	0.91	1.19
Average	130.00	0.80	170.74	1.05	1.06	1.37
St.Dev.	26.46	0.16	28.83	0.18	0.18	0.21
Median	120.00	0.74	163.79	1.01	1.02	1.32
Worldwide	60.00	1.00	60.00	1.00	< 1.00	< 1.00

The *In Situ* obtained values of the absorbed dose rate in air at 1 m above the ground surface measured at different sampling points varied from 50.00 to 90.00 nGy/h with a mean value of 73.00 nGy/h in Fongo-Tongo and from 110.00 to 160.00 nGy/h with an average 130.00 nGy/h in Mini-matap while the calculated value of absorbed dose rate in air at 1 m above the ground level obtained from the different sampling points based on the specific activity concentrations of <sup>226</sup>Ra, <sup>232</sup>Th and <sup>40</sup>K measured in samples from Fongo-Tongo and Mini-matap ranged from 92.91 to 188.76 nGy/h with an average of 127.42 nGy/h and from 146.03 to 202.47 nGy/h with a mean of 170.74 nGy/h, respectively as shown in Table 2. The obtained average values in Fongo-Tongo and Mini-matap by *In-situ* and calculation based on Equation (3) are higher than the worldwide average value of 60.00 nGy/h UNSCEAR [20].

The *In Situ* annual effective dose to which population are exposed to in Fongo-Tongo and Mini-matap ranged from 0.31 to 0.55 mSv/year with a mean of 0.45 mSv/year and from 0.67 to 0.98 mSv/year with average of 0.80 mSv/year, respectively. The estimated annual effective dose to which population are likely be exposed in the study sites ranged from 0.50 to 1.26 mSv/year with a mean value of 0.76 mSv/year in Fongo-Tongo and from 0.90 to 1.24 mSv/year

with a mean of 1.05 mSv/year in Mini-matap. The obtained average values in Fongo-Tongo and Mini-matap in *In-situ* and calculation were lower than the safe limit of 1.00 mSv/year recommended by UNSCEAR [20] except that of Mini-matap where the average values were slightly higher than the safe values.

Comparing the *In Situ* and the calculation value of the absorbed dose rate in air at 1 m above the ground level and the annual effective dose to which population may likely be exposed at different sampling points in both study sites are shown in Figs. 1 and 2. The recorded values for the *In situ* are lower than the calculated values at different sampling points except that of sample "MT3" with *In-Situ* values for both hazards parameters higher than the calculated values.

The hazard indices parameters calculated to assess the level of risk to which the population may be exposed to the terrestrial radiation from soil are shown in Table 2. The obtained values of external index ranged from 0.50 to 1.16 with an average of 0.78 in Fongo-Tongo and from 0.90 to 1.24 with a mean of 1.07 in Mini-matap. The internal hazard index values in Fongo-Tongo and Mini-matap varied from 0.69 to 1.64 with a mean of 1.06 and from 1.19 to 1.60 with an average of 1.37, respectively.

**Table 3. Comparison of specific gamma activities (Bq/kg) in soil with that of other countries**

Country	Activity concentration (Bq/kg)			References
	Ra-226	Th-232	K-40	
China (Xiaz-hung area)	40.2-442(112)	32.6-88.1(71.5)	440-913(672)	Yang et al. [23]
Botswana	6.1-97.4(34.8)	7.4-110.0(41.8)	33.5-1085.7(432.7)	Murty, Karanick [22]
Ghana (Great Accra)	2.4-62.7	3.2-145.7	91.1-1395.9	Yeboah et al. [25]
India (Himwchal Pradesh)	42.09-79.63(57.34)	52.83-135.75(82.22)	95.33-160.30(135.75)	Asha Rani, Surinder Singh [26]
East Rhodopes	8-67	20-109	539-859	Hristov et al [24]
Italy (Southern)	57-71	73-87	580-760	Bellia et al. [27]
Namibia	4.5-48(31)	3-38(32)	42-1100(480)	Steinhauser and Lettner [28]
Nigeria Delta	11-40 (18±3.4)	12-40(22±4.4)	69-530(210±49)	Agbalagba, Onga [29]
Cameroon	21.98-29.16(25.475)/	59.13-65.87(65.95)/	13.927-70.886(39.147)/	Ndontchueng et al.[12]
(CampusI/CampusII)	21.99-27.68 (24.50)	52.59-78.99(66.717)	11.885-80.763(28.185)	
Cameroon	56.56-176.14(108.91)/	82.54-177.78 (117.79)/	BDL-1379.62±37.22	Present work
(Fongo-Tongo/Mini-Matap)	102.69-124.41(113.15)	163.22-239.96 (196.14)	(143.07)/ BDL	



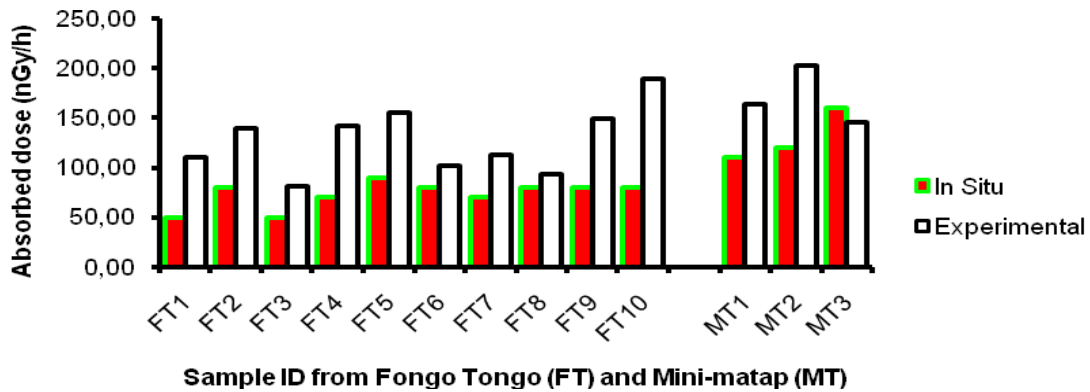


Fig. 1. Comparison of *In-situ* and experimental values of absorbed dose at 1 m above the ground in soil samples from Fongo-Tongo and Mini-matap

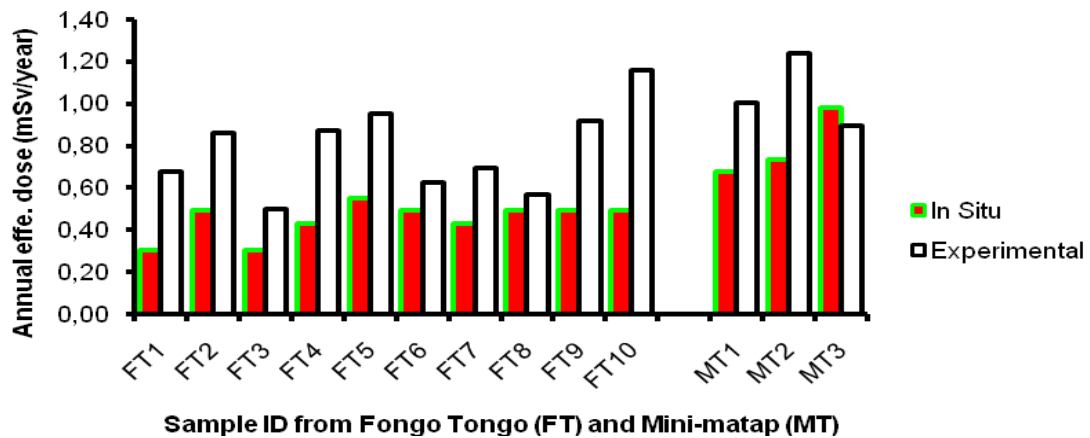


Fig. 2. Comparison of *In-situ* and experimental values of the annual effective dose equivalent in soil samples from Fongo-Tongo and Mini-matap

Comparing the obtained average values of both external and internal hazard indices in both areas, it can be seen that the obtained average values of both hazard parameters in Fongo-Tongo were lower than the safe limits values except for the internal hazard index value which were slightly higher than the recommended average values by UNSCEAR [20].

#### 4. CONCLUSION

The investigation of NORMs and some related health hazard parameters in soil samples from Fongo-Tongo and Mini-matap (bauxites deposition areas) has been carried out using gamma spectrometry and dose rate survey manufacturer by CANBERRA.

The average values of  $^{226}\text{Ra}$ ,  $^{232}\text{Th}$  and  $^{40}\text{K}$  in the soil samples from Fongo-Tongo and Mini-Matap

were 108.91 Bq/kg, 117.79 Bq/kg and 143.07 Bq/kg and, 113.15Bq/kg, 196.14 Bq/kg and zero, respectively. These values were higher than the safe limits recommended values by UNSCEAR [20] except that of  $^{40}\text{K}$ . The absorbed dose rate at 1 m above the ground and the annual effective dose equivalent obtained for the *In-situ* were lower than the obtained values from the specific activity of  $^{226}\text{Ra}$ ,  $^{232}\text{Th}$  and  $^{40}\text{K}$ . The average external and internal hazard indices in samples were 0.78 and 1.06 in Fongo-Tongo and, 1.07 and 1.37 in Mini-matap. The internal and external hazard indices are comparably higher than the worldwide safe values except the average external hazard index obtained in Fongo-Tongo.

The results in this study present higher radioactivity of NORM than the global safe limits recommended by UNSCEAR [20]. Stakeholders could use the findings of this study as a data

bank in formulating regulations for NORM in soil to ensure adequate safety of population. Since study covers only a specific bauxite site in West Region of Cameroon, it is recommended that further investigations should be done in other mining sites.

## ACKNOWLEDGMENTS

The authors are grateful for the support and technical cooperation provided by the National Radiation Protection Agency of Cameroon in granting access to the facilities to successfully complete this study. The authors also appreciate the community of Fongo-Tongo and Mini-Matap for the understanding during sampling period; they also wish to thank Dr. Tchoffo, Lecturer at the Faculty of Sciences of the University of Dschang for his understanding and availability to direct us during sampling period.

## COMPETING INTERESTS

The authors declare no to have any conflict of interests regarding the publication of this paper.

## REFERENCES

- Bardossy G. Aleva, Geol G, Lateritic JJ. Developments in economic bauxites, Deogy, Elsevier, Amsterdam. 1990;27:624.
- Lee Bray E. US geological survey, mineral commodity summaries, United States Government Printing Office, Washington; 2009.
- Kobilseck B. Geochemistry and petrology bauxite lateritic Brazilian Amazon, Comparison Avec l'Afrique, India and Australia. Thesis University Louis Pasteur, Strasbourg; 1990.
- Edlinger W. Contribution to geology and petrography mawa, Ph.D. Thesis, Erlangen Uni- of the German Adaversity, Erlangen. 1908;125.
- Passarge S. The superficial structure and geology of Cameroon. Annual Review of German Colonies. 1910;448-465.
- Weeksteen. Preliminary report on the Fongo Tongo Bauxite ore Deposits. Report of the Mine and Geology of the Cameroon State; 1957.
- Eno Belinga SM. The alteration of basalt rocks and process bauxitisation in Adamawa (Cameroon), "PhD Thesis State University Paris Sud-IV, Paris. 1972;571
- Hieronimus B. Study of the weathering of eruptive rocks in the West Cameroon. Earth Sciences Thesis. University of Paris VI, Paris. 1985;85.
- Sojien M. Petrographic study, mineralogy and geochemistry of bauxite training Bangamdans of the High West Cameroon. Thèse MSc., Université Dschang, Dschang. 2007;77.
- Nyobe JB. A geological and geochemical of the Fongo-Tongo and areally related bauxite deposits. PhD Thesis, Werstern Highlands, Cameroon; 1987.
- Ndontchueng MM, Njinga RL, Nguelem EJM, Simo A. Analysis of  $^{238}\text{U}$ ,  $^{235}\text{U}$ ,  $^{137}\text{Cs}$ ,  $^{133}\text{Xe}$  in soils from two campuses in university of Douala-Cameroon. Applied Radiation and Isotopes 86. 2014;85-89.
- Ndontchueng MM, Nguelem EJM, Njinga RL, Simo A, Guembou JCS. Gamma emitting radionuclides in soils from selected areas in Douala-Bassa zone, littoral region of Cameroon. ISRN Spectroscopy. 2014;(2014):8. Article ID 245125.
- Momo MN, Tematio P, Yemefack M. Multi-scale organization of the Doumbouo-Fokoué bauxites ore deposits (West Cameroon): Implication to the Landscape Lowering. Open Journal of Geology. 2012;(2):14-24.
- European Commission. Radiation protection 112-radiological protection principles concerning the natural radioactivity of building materials directorate-general environment. Nuclear safety and civil Protection; 1999.
- Xinwei L. Natural radioactivity in some building materials of shaanix, China. J. Radioanaly. Nucl. Chemi. 2004;262:775-777.
- Beretka I, Mathew PI. Natural radioactivity of Australian building materials, waste and by products, Health Physics. 1985;48:87-95.
- Damla N, Cevik U, Kobya AI, Celik A, Celik N, Van Grieken R. Radiation dose estimation and mass attenuation coefficients of cement samples used in Turkey. J. Hazardous Materials. 2010;176:644-649.
- Al-Hamarneh IF, Awadallah MI. Soil radioactivity levels and radiation Hazard Assessment in the Highlands of Northern Jordan. Radiation Measurements. 2009;44:102-110.

19. Krieger R. Radioactivity of construction materials. *Betonwerk Fertigteile* Tech. 1981;47:468-473.
20. United Nations Scientific Committee on the Effect of Atomic Radiation (UNSCEAR), Report to the General Assembly. Annex B: Exposures from Natural Radiation Sources; 2000.
21. Turhan S, Gundiz L. Determination of specific activity of  $^{226}\text{Ra}$ ,  $^{232}\text{Th}$  and  $^{40}\text{K}$  for assessment of radiation Hazards from Turkish Pumice Samples. *Journal of Environmental Radioactivity*. 2008;99:332-342.
22. Murty VRK, Karunakara N. Natural radioactivity in the soil sample of Botswana. *Radiation Measurements*. 2008;48:1541-1545.
23. Yang, Ya-Xin, Xin-min, Wu, Zong-ying, Jiang, Wei-Xing, Wang, Ji-gen, Lu, Jun, Lin, Lei-Ming, Wang, Yuang-fu, Hsia. Radioactivity concentrations in soils of Xiaz-hung granite area, China. *Journal of Applied Radiation and Isotopes*. 2005;63:255-259.
24. Hristov HR, Marinova S, Aladjadjian A, Gorbanov ST. Measuring the content of Natural Technological Radionuclides in soils from mining regions in East Rhodopes. *J. Environ. Prot. & Ecol*. 2004;5(2):448-450.
25. Yeboah J, Boadu M, Darko EO. Natural radioactivity in soils and rocks within the greater Accra Region of Ghana. *Journal of Radioanalytical and Nuclear Chemistry*. 2011;249(3):629-632.
26. Rani A, Singh S. Natural radioactivity levels in soil samples from some areas of Himachal Pradesh, India using  $\gamma$ -ray spectrometry. *Atmospheric Environment*. 2005;39(34):6306–6314.
27. Bellia S, Brai M, Hauser S, Puccio P, Rizzo S. Natural radioactivity in a Volcanic Island: Ustica, Southern Italy. *Applied Radiation and Isotopes*. 1997;48(2):287–293.
28. Steinhausler F, Lettner H. Radiometric survey in Namibia. *Radiation Protection Dosimetry*. 1992;45(1-4):553–555.
29. Agbalagba EO, Onoja RA. Evaluation of natural radioactivity in soil, sediment and water samples of Niger Delta (Biseni) flood plain lakes, Nigeria. *Journal of Environmental Radioactivity*. 2011;102(7): 667–671.

© 2015 Ndontchueng et al.; This is an Open Access article distributed under the terms of the Creative Commons Attribution License (<http://creativecommons.org/licenses/by/4.0>), which permits unrestricted use, distribution, and reproduction in any medium, provided the original work is properly cited.

*Peer-review history:*

*The peer review history for this paper can be accessed here:*  
<http://www.sciencedomain.org/review-history.php?iid=761&id=5&aid=6644>